Equilibrium of Oxygen Sorption on Perovskite-Type Lanthanum Cobaltite Sorbent

Zhaohui Yang and Y. S. Lin
Dept. of Chemical Engineering, University of Cincinnati, Cincinnati, OH 45221

Perovskite-type oxides are a group of ceramic compounds having the general formula of ABO_3 with a simple cubic crystal structure. Perovskite-type ceramics have attracted increasing interests since the 1940s. Among perovskite-type ceramics, lanthanum cobaltite series has recently received increasing attention, mainly for membranes separation and membrane reactor applications. Several groups have studied oxygen defect chemistry, oxygen ionic and electronic conductivities, oxygen permeability, and oxygen surface exchange rates (van Hassel et al., 1993; Bouwmeester et al., 1994; Ma et al., 1996; Liu et al., 1996; Chen et al., 1997; Zeng and Lin, 1998; Zeng et al., 1998). Membranes made of this group of perovskite-type ceramics offer very high oxygen permeability with infinite selectivity for oxygen. Despite their many inherent advantages for air separation and membrane reactor applications, perovskite-type ceramic based membrane processes still face many technical challenges (Dyer et al., 2000; Lin, 2001) such as chemical and structural instability of the perovskite membrane and the complexity of designing and fabricating large-scale dense membrane modules and a process that can ensure safe operation. Nevertheless, recent studies on these perovskite-type ceramic membranes have provided much useful information that leads to the following new concept of high temperature sorption processes for air separation.

Recently, Lin and coworkers (Lin et al., 2000; Yang et al., 2002) reported a new application of the perovskite-type ceramics as sorbents in high-temperature sorption processes for air separation and oxygen removal. The high-temperature sorption processes are based on the fact that the oxygen nonstoichiometry δ for a doped perovskite type ceramic ($A_{1-x}A'_xB_{1-y}B'_yO_{3-\delta}$) is a function of temperature and oxygen partial pressure. By changing temperature or oxygen partial pressure, oxygen nonstoichiometry, or oxygen content in the solid, changes. Within a certain range of temperature and oxygen partial pressure, the change of the oxygen nonstoichiometry does not affect its perovskite structure, and the change of the oxygen content in the material is reversible. Yang et al. (2002) reported that, at high temperature (600°C), a lanthanum cobaltite sorbent can adsorb oxygen up to 0.6 mmol/g with zero sorption for nitrogen. The oxygen sorption capacity of the perovskite-type ceramics at high temperature is comparable to the nitrogen sorption capacity of LiX zeolite (Rege et al., 1997). However, the former is oxygen selective with an infinite oxygen to nitrogen selectivity, and the latter is nitrogen selective with a maximum nitrogen to oxygen selectivity of around 10. Yang et al. (2002) showed that the perovskite-type ceramics are potentially excellent sorbents for adsorption processes for air separation and oxygen removal.

In comparison with perovskite-type ceramic membrane separation process, the high-temperature oxygen sorption processes would not have the sorbent stability problem and do not require a seal. Furthermore, sorption technology (sorbent and adsorber fabrication, and design, manufacturing and operation of large-scale sorption processes) is well established as compared to the high-temperature membrane technology. These will make such high-temperature sorption processes more attractive from an industrial viewpoint. To develop these high-temperature oxygen sorption separation processes, a systematic investigation is required to study the oxygen sorption equilibrium and kinetic properties on this group of new sorbents. This article reports results of a theoretical and experimental study on oxygen nonstoichiometry, oxygen sorption isotherms, and the heat of sorption of a representative perovskite-type ceramic sorbent $La_{0.1}Sr_{0.9}Co_{0.5}Fe_{0.5}O_{3-\delta}$ (LSCF).

Modeling Oxygen Sorption Equilibrium

A point defect model has been successfully applied to several lanthanum cobaltite perovskite-type materials with lower Sr dopant (Mizusaki et al., 1984, 1985, 1989; van Roosmalen et al., 1991; van Hassel et al., 1993). For the present lanthanum cobaltite ($La_{0.1}Sr_{0.9}Co_{0.5}Fe_{0.5}O_{3-\delta}$) with large Sr doping amount and two metal species on B-site, the cluster defect model (van Roosmalen et al., 1991; van Hassel et al., 1993; Yasuda and Hishinuma, 1996) should work better. Therefore, we present the cluster defect model below for the present lanthanum cobaltite.

To simplify the model, we assume that both B- site ions (Co, and Fe) have similar reactivity. There are two forms of

Correspondence concerning this article should be addressed to Y. S. Lin.

oxygen vacancies present in the material: one is randomly distributed oxygen vacancy, and the other is oxygen vacancy in a certain ordered cluster structure. Randomly distributed oxygen vacancy is formed by a defect reaction described as (in Kroger-Vink notations)

$$2B_B^{\bullet} + O_O^x \Leftrightarrow 2B_B^x + V_O^{\bullet\bullet} + \frac{1}{2}\mathrm{O}_2(g) \qquad \text{(A)}$$

The following equilibrium relation holds for reaction A

$$K_1 = \frac{[B_B^x]^2[V_{\mathrm{O}}^{\bullet\bullet}]P_{\mathrm{O}_2}^{1/2}}{[B_B^{\bullet}]^2[O_O^x]} \qquad (1)$$

where K_1 is the defect reaction equilibrium constant. The cluster oxygen defect is in the form of a certain cluster structure with the combination of B-site ions. For our material, the cluster defect could be induced from the shift of valance on B-site ions, in which two B_B^X cations transform into B'_B and form a neutral cluster structure with oxygen vacancy as $[B'_B - V_O^{\bullet\bullet} - B'_B]$, and the defect reaction is given by

$$2B_B^X + O_o^X \Leftrightarrow [B'_B - V_o^{\bullet\bullet} - B'_B] + \frac{1}{2}O_2 \qquad (B)$$

For reaction B, the formation of a cluster defect, the reaction equilibrium constant at a given temperature K_2, is defined as

$$K_2 = \frac{[B'_B - V_O^{\bullet\bullet} - B'_B]P_{\mathrm{O}_2}^{1/2}}{[B_B^X]^2[O_O^X]} \qquad (2)$$

Three other equations can be derived from mass balance on the B-site species, charge neutrality of the system, and oxygen stoichiometry. These equations are in the similar forms as those published in literature (van Roosmalen et al., 1991; van Hassel et al., 1993). These five equations form a set of nonlinear equations which include five unknowns, the concentrations of the defects in the perovskite-type ceramic crystals, $[B_B^{\bullet}]$, $[B_B^X]$, $[B'_B - V_O^{\bullet\bullet} - B'_B]$, $[O_O^X]$, $[V_O^{\bullet\bullet}]$. K_1 and K_2 can be obtained by regressing experimental data with above five equations. The simultaneous solution of these five equations will give dependency of the oxygen vacancy concentration and other defect concentrations on oxygen partial pressure. The Microsoft IMSL subroutine NEQBF was used to solve these nonlinear equations using factored secant update with a finite-difference approximation to the Jacobian.

Experimental Section

$La_{0.1}Sr_{0.9}Co_{0.5}Fe_{0.5}O_{3-\delta}$ (LSCF) powder was prepared by liquid citrate method followed by firing at 1250°C for 25 h (Zeng et al., 1998; Yang et al., 2002). High-temperature firing ensured the formation of a perovskite-type crystallographic structure. The perovskite-type crystalline structure of the LSCF sample was confirmed by XRD pattern (CuKα_1). Scanning electronic microscopic (Hitachi S-4000) analysis revealed that the LSCF powder contained approximately spherical dense particles of about 180 μm in diameter. The average density of the LSCF powder was 5.7 g/cm^3.

Oxygen nonstoichiometry δ which can be directly related to oxygen vacancy concentration or oxygen sorption capacity, was experimentally determined by the gravimetric method (Zeng and Lin, 1998; Yang et al., 2002). These measurements were conducted on a Cahn electronic-microbalance (Cahn-1000), and a description of the experimental setup was given elsewhere (Zeng and Lin, 1998). Details on experimental procedure and determination of oxygen nonstoichiometry were given elsewhere (Yang et al., 2002).

Heat of sorption is one of the most important properties of adsorbents. One of the objectives of this work is to estimate the heat of sorption on this new type of adsorbent for oxygen sorption. Isosteric heat of oxygen sorption was calculated from oxygen nonstoichiometry data at different temperatures and oxygen partial pressures. Apparent heats of sorption were also determined by simultaneous DSC-TGA measurement (TA Instruments, SDT-2960). During the experiment, about 20–30 mg sorbent material was put in the alumina sample pan in the DSC-TGA instrument. The sample was first exposed to a flow of dry nitrogen (99.999% purity) at a flow rate of 100 mL/min. At the steady state, the nitrogen flow was switched to dry air flow at the same flow rate. The percentage of the weight change w was obtained from the TGA curve, and the integrated heat amount Q was obtained by integrating DSC curve (heat flux vs time). The apparent heat of sorption of the sample corresponding to a switch of the surrounding atmosphere from nitrogen to air at a given temperature was then calculated by the following equation

$$H_{\mathrm{app}} = \frac{Q}{w} \times M_{\mathrm{O}_2} \times CF \qquad (3)$$

where M_{O2} is the molecular weight of oxygen and CF is the calibration factor of the DSC-TGA system. To obtain an accurate calibration factor, the melting heat of three metals, aluminum, zinc, and silver, having melting points of 692.78 K, 933.5 K and 1235.1 K respectively, was measured and compared with the literature heat of fusion. The average calibration factor obtained for the TGA-DSC instrument was 0.974.

Results and Discussion

Oxygen nonstoichiometry and its comparison with models

Figure 1 shows the comparison of oxygen nonstoichiometry determined by experimental measurements and cluster model. In the temperature and P_{O2} ranges of the investigation, the cluster defect model agrees well with the experimental data. Generally, oxygen nonstoichiometry decreases with decreasing temperature and increasing P_{O2} in the ambient gas phase. As seen from the figure, oxygen nonstoichiometry exhibits nearly logarithmic dependence on the oxygen partial pressure in the temperature range studied.

The values of the two reaction equilibrium constants, K_1 and K_2 in the simple cluster model obtained by the regression are listed in Table 1. Figure 2 shows Arrhenius plots of the reaction equilibrium constants K_1 and K_2 based on the cluster defect model. The negative slopes indicate that both reaction A and reaction B are endothermic. This is expected

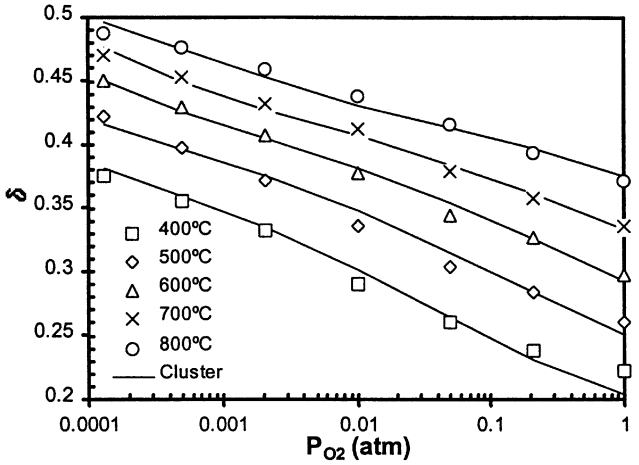

Figure 1. Experimental data (points) and model fit for oxygen nonstoichiometry at different P_{O_2} at temperatures.

since the formation of oxygen vacancy or defect can be considered as a desorption process, which is normally endothermic. The heat of reaction calculated from the Arrhenius plots is 59.7 kJ/mol and 55.5 kJ/mol, respectively, for reaction A and B.

Once constants K_1 and K_2 are determined, the concentrations of various defects were calculated from the simple cluster model at different temperatures and oxygen partial pressures. Figure 3 shows the distribution of the randomly distributed oxygen defect $[V_O^{\bullet\bullet}]$ and cluster oxygen defect $[B'_B - V_O^{\bullet\bullet} - B'_B]$, as a function of P_{O2}, at 400°C and 800°C. As seen from the figure, with the increase of P_{O2}, both random and cluster oxygen defects decrease. This is also true for other temperatures. At 400°C, the concentration of cluster vacancy is negligible in the P_{O2} range studied, but becomes appreciable at higher temperatures. For example, at 800°C in He (P_{O2} of 1.3×10^{-4} atm), the oxygen vacancy δ in cluster is 0.0655. Therefore, the cluster defects can be important at higher temperatures.

Reaction equilibrium constant K_1 is several orders of magnitude higher than K_2, suggesting that reaction A is thermodynamically more favorable than reaction B. It is more likely that $La_{0.1}Sr_{0.9}Co_{0.5}Fe_{0.5}O_{3-\delta}$ (LSCF), simplified as $La_{0.1}Sr_{0.9}BO_{3-\delta}$, should have a composition of $La_{0.1}Sr_{0.9}(B_B^{\bullet})_{0.9}(B_B^X)_{0.1}O_3$ stoichiometric condition due to the charge balance and the fact that A-site cations have fixed valances and B-site cations have variable valances. Mixed valance on B-site cation(s) plays a very important role in the formation of oxygen vacancy in perovskite-type ceramics at elevated temperatures. The random oxygen defects are

Table 1. K_1 and K_2 in Cluster Defect Modeling

Temp. (°C)	K_1 (atm$^{1/2}$)	K_2 (atm$^{1/2}$)
400	0.062	1.07×10^{-5}
500	0.190	5.64×10^{-5}
600	0.510	1.58×10^{-4}
700	1.323	2.53×10^{-4}
800	3.531	4.58×10^{-4}

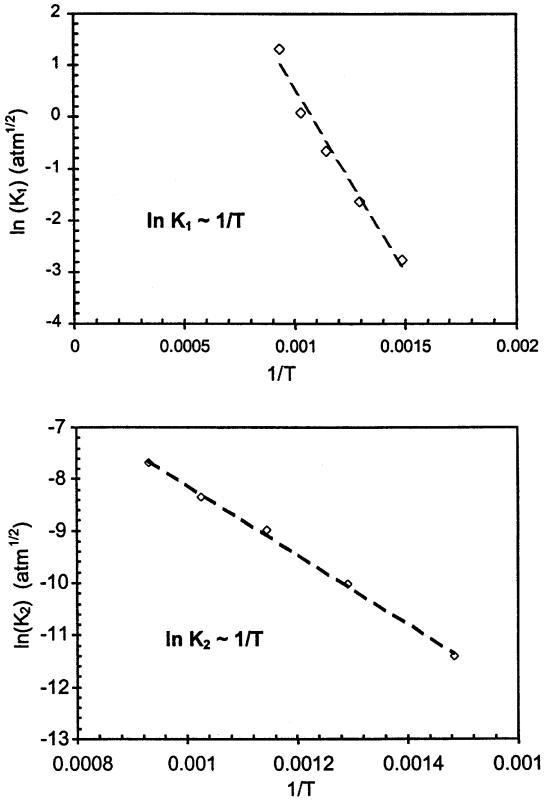

Figure 2. Two reaction equilibrium constants in the cluster defect model at different temperatures.

formed to compensate the shift of the B-site valance from $[B_B^{\bullet}]$ to $[B_B^X]$, and the cluster oxygen defects are formed due to the shift of the B-site valence from $[B_B^X]$ to $[B'_B]$. Oxygen defect concentration increases with increasing temperature and/or decreasing P_{O2}. Due to the large amount of $B_B^{\bullet}$ (mole fraction of 90%) in the stoichiometric condition, these defects formed are initially the random ones due to the reduction of $B_B^{\bullet}$ to B_B^X, with negligible the cluster defects. When the mole fraction of B_B^X increases and P_{O2} in the gas-phase decreases to a certain extent, the formation of the cluster defect becomes important, as shown in Eq. 2.

Oxygen sorption isotherms and heat of sorption

Oxygen sorption isotherms on the perovskite-type oxide was determined from the oxygen nonstoichiometry at different oxygen partial pressures and constant temperature. Different from other conventional sorbents (such as zeolites and carbon molecular sieves) for oxygen sorption, the oxygen content in the perovskite-type ceramics may change even at very low oxygen partial pressure range. A reference state, corresponding to the conditions where the sorbent is regenerated, should be selected. In this study, P_{O2} of 1.3×10^{-4} atm was selected as the reference state. The oxygen sorption isotherm of the LSCF sample at different temperatures were calculated by the following equation

$$q = \frac{-\Delta\delta/2}{\bar{M}_w} \tag{4}$$

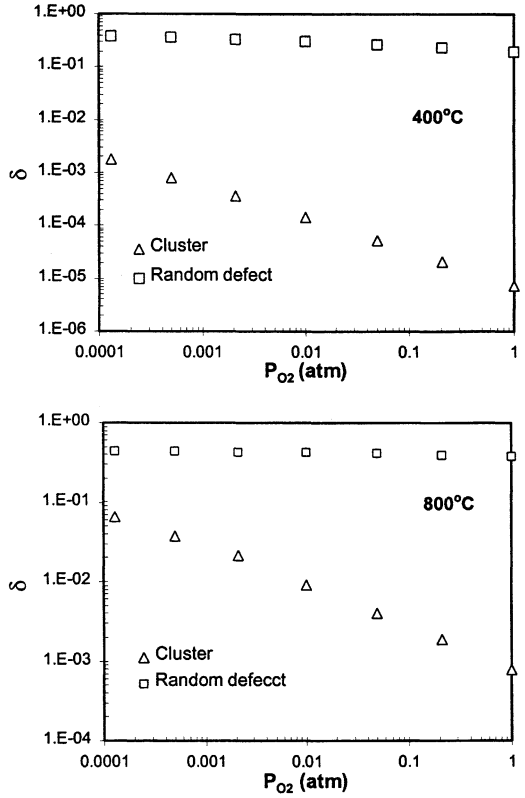

Figure 3. Distribution of oxygen defects with P_{O_2} at different temperatures.

where q is the sorption capacity (mol/g adsorbent), $\Delta\delta$ is the difference of oxygen nonstoichiometry between a given P_{O2} and the reference P_{O2} (1.3×10^{-4} atm, or He), and $\overline{M}_w$ is the average molecular weight of the sorbent during the sorption process.

Experimental data of oxygen sorption isotherms for the LSCF sample are presented in Figure 4. For this LSCF sample, oxygen sorption capacity follows approximately linear dependency on $\log(P_{O2})$, which is determined by the shape of $\delta - P_{O2}$ curve shown in Figure 1. Above 500°C, the sorption capacity decreases with increasing temperature, while a contradictory trend is seen between 400 and 500°C. As stated above, oxygen nonstoichiometry always increases with increasing temperature. However, oxygen sorption capacity is proportional to the difference of oxygen nonstoichiometry between a given P_{O2} and the reference condition $P_{O2} = 1.3\times10^{-4}$ in this case. For this specific perovskite-type ceramic LSCF, this difference at 400°C is slightly lower than that at 500°C, as shown in Figure 1; this explains the seemingly "contradictory trend" at 400 and 500°C. It should be noted that the sorption capacity for the perovskite type ceramic sorbent is fairly high even at such high temperatures. These values are comparable to nitrogen sorption capacity of zeolite LiX at room temperature (Yang et al., 2002).

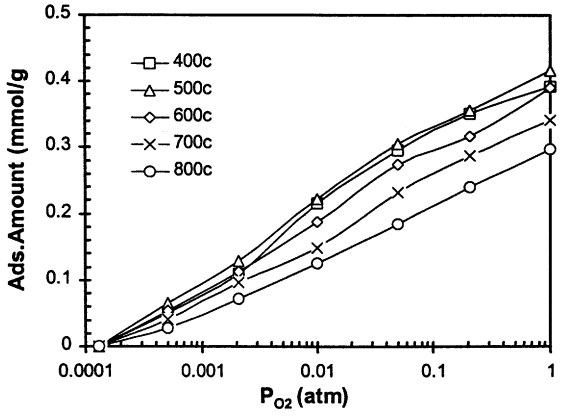

Figure 4. Oxygen sorption isotherms of LSCF.

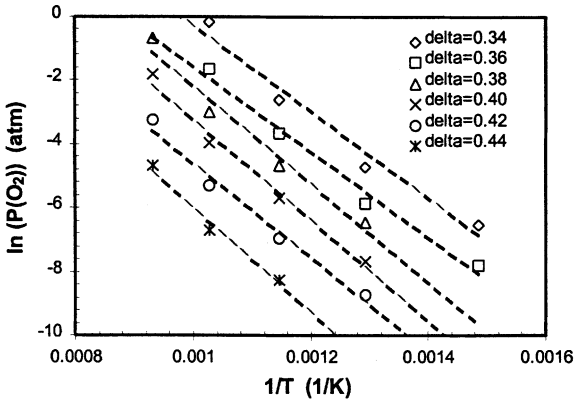

Figure 5. Calculation of isosteric heat of sorption of LSCF (points are experimental data).

In this work, the heat of sorption was first obtained by the isosteric method, and the relationship is expressed in the following equation

$$h_o - h_o^0 = \left(\frac{R}{2}\right)\left[\frac{\partial \ln P_{O2}}{\partial(1/T)}\right] \tag{5}$$

Regression of the straight lines of the plots of $\ln P_{O2} \sim 1/T$ in Figure 5 gave the slopes from which the isosteric heat of sorption was calculated. For the LSCF sample, the isosteric heat of sorption obtained is in the range of 108–133 kJ/mol. These data of isosteric heat of sorption are also consistent with the modeling results described above. In the simple cluster model, the heats of reaction are 59.7 kJ/mol and 55.5 kJ/mol for the formation of random and cluster oxygen vacancy, respectively. These values are translated to 119.4 kJ/mol and 110.0 kJ/mol based on a unit mole of the molecular oxygen. A lower isosteric heat of sorption suggests a weaker bonding of oxygen with the metal ions on the LSCF sample studied. B-site doping amount has a marked effect on the properties of adsorbed oxygen, especially the bonding strength (Zhang et al., 1989, 1990). Therefore, it is possible to tailor the properties of the heat of sorption of the perovskite materials by controlling B-site composition.

The apparent heat of sorption for the LSCF sample was also measured by the DSC-TGA method. Typical simultaneous DSC-TGA curves are given in Figure 6. By using Eq. 3, the apparent heat of sorption was calculated as 104.9 kJ/mol

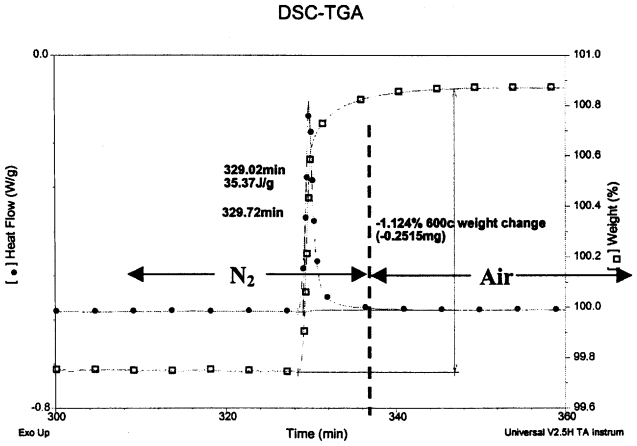

Figure 6. Representative data for simultaneous DSC-TGA measurement of oxygen sorption on LSCF at 600°C.

at this temperature. The apparent heats of sorption at other temperatures were also obtained and the results are given in Table 2. As seen from the table, from 400°C to 750°C, the apparent heat of sorption is in the range of 98.5 to 121.0 kJ/mol. The apparent heat of sorption decreases with increasing temperature. We believe this is due to the fact that the heat capacities of reactants and products change with temperature. In the broad range of the temperature (400–750°C) in this work, it is not surprising to observe the change of heat of sorption with temperature. Although the heat of sorption can be modified by controlling the material composition, a good heat management is essential to the design of a sorption process based on this group of ceramic sorbents.

Conclusions

Oxygen nonstoichiometry and heat of sorption of a perovskite-type ceramic $La_{0.1}Sr_{0.9}Co_{0.5}Fe_{0.5}O_{3-\delta}$ (LSCF) was investigated in this work. The material exhibits large changes of oxygen defect with respect to temperature and oxygen partial pressure. As a result, this material offers a large capacity for oxygen sorption at high temperatures. Sorption isotherms of the material at different temperatures are obtained from the oxygen nonstoichiometry δ data.

A simple cluster model was used to describe oxygen sorption equilibrium for this perovskite-type ceramic sorbent. The model fits the experimental data well. Isosteric heat of oxygen sorption calculated from the oxygen nonstoichiometry data for this material is in the range of 108–133 kJ/mol. The apparent heat of oxygen sorption measured by TGA-DSC is in the range of 99–120 kJ/mol and increases with decreasing temperature. These heat of oxygen sorption data agree with the heat of reaction for the formation of oxygen vacancy based on the simple cluster defect model. The heat of oxygen sorption in this group of ceramics is significantly larger than the heat of physical adsorption of oxygen.

Table 2. Apparent Heat of Sorption at Various Temperatures by DSC-TGA

T (°C)	Q (J/g Sorbent)	wt. %	Heat of Sorption (kJ/mol)
400	37.48	1.016	120.95
450	41.02	1.113	120.84
500	40.52	1.192	112.37
550	40.69	1.202	111.91
600	35.37	1.124	104.90
650	33.91	1.099	102.85
700	28.39	0.9604	98.54
750	27.54	0.8928	101.55

Acknowledgments

We would like to acknowledge the support of the NSF (CTS-0132684) and the BOC Group on the work reported in this article.

Literature Cited

Bouwmeester, H. J. M., H. Kruidhof, and A. J. Burggraaf, "Importance of the Surface Exchange Kinetics as Rate-Limiting Step in Oxygen Permeation Through Mixed-Conducting Oxides," *Solid State Ionics*, **72**, 185 (1994).

Burggraaf, A. J., and L. Cot, *Fundamentals of Inorganic Membrane Science and Technology*, Elsevier Science, New York (1996).

Chen, C. H., H. J. M. Bouwmeester, R. H. E. van Doorn, H. Kruidhof, and A. J. Burggraaf, "Oxygen Permeation of $La_{0.3}Sr_{0.7}CoO_{3-\delta}$," *Solid State Ionics*, **98**, 7 (1997).

Goldschmidt, V. M., "Geochemische Verteilungsgesetez der Elemente VII," *Skrif. Nor. Vidensk Akad. Mat. Natur. Oslo. I.*, **8**, 7 (1926).

Dyer, P. N., R. E. Richards, S. L. Russek, and D. M. Taylor, "Ion Transport Membrane Technology for Oxygen Separation and Syngas Production," *Solid State Ionics*, **134**, 21 (2000).

Lin, Y. S., "Microporous and Dense Inorganic Membranes, Current Status and Prospecties," *Separ. Purif. Technology*, in press (2001).

Lin, Y. S., D. L. Maclean, and Y. Zeng, "High Temperature Adsorption Process," US Patent No. 6059858 (2000).

Liu, L. M., T. H. Lee, L. Qiu, Y. L. Yang, and A. J. Jacobson, "A Thermogravimetric Study of the Phase Diagram of Strontium Cobalt Iron Oxide, $SrCo_{0.8}Fe_{0.2}O_{3-\delta}$," *Mater. Res. Bull.*, **31**, 29 (1996).

Ma, B., U. Balachandran, J. H. Park, and C. U. Segre, "Determination of Chemical Diffusion Coefficient of $SrFeCo_{0.5}O_x$ by the Conductivity Relaxation Method," *Solid State Ionics*, **83**, 65 (1996).

Mizusaki, J., S. Yamauchi, K. Fueki, and A. Ishikawa, "Nonstoichiometry of Perovskite-Type Oxides $La_{1-x}Sr_xCoO_{3-\delta}$, *Solid State Ionics*, **12**, 119 (1984).

Mizusaki, J., M. Yoshihiro, S. Yamauchi, and K. Fueki, "Nonstoichiometry and Structure of Perovskite-type Oxides $La_{1-x}Sr_xFeO_{3-\delta}$," *J. Solid State Chem.*, **58**, 257 (1985).

Mizusaki, J., Y. Mima, S. Yamauchi, K. Fueki, and H. Tagawa, "Nonstoichiometry of the Perovskite-Type Oxides $La_{1-x}Sr_xCoO_{3-\delta}$," *J. Solid State Chem.*, **80**, 102 (1989).

Rege, S. U., and R. T. Yang, "Limit for Air Separation by Adsorption with LiX Zeolite," *Ind. Eng. Chem. Res.,* **36**(12), 5358 (1997).

van Hassel, B. A., T. Kawada, N. Sakai, H. Yokokawa, M. Dokiya, and H. J. M. Bouwmeester, "Oxygen Permeation Modeling of Perovskites," *Solid State Ionics*, **66**, 295 (1993).

van Roosmalen, J. A. M., and E. H. P. Cordfunke, "A New Defect Model to Describe the Oxygen Deficiency in Perovskite-Type Oxides," *J. Solid State Chem.*, **93**, 212 (1991).

Yang, Z. H., Y. X. Zeng, and Y. S. Lin, "High-Temperature Sorption for Air Separation," *Ind. Eng. Chem. Res.*, **41**, 2775 (2002).

Yasuda, I., and M. Hishinuma, "Electrical Conductivity and Chemical Diffusion Coefficient of Strontium-Doped Lanthanum Manganites," *J. Solid State Chem.*, **123**, 382 (1996).

Zeng, Y., and Y. S. Lin, "A Transient TGA Study on Oxygen Permeation Properties of Perovskite-type Ceramic Membrane," *Solid State Ionics*, **110**, 209 (1998).

Zeng, Y., Y. S. Lin, and S. L. Swartz, "Perovskite-Type Ceramic Membrane: Synthesis, Oxygen Permeation and Membrane Reactor Performance for Oxidative Coupling of Methane," *J. Membr. Sci.*, **150**, 87 (1998).

Zhang, H. M., N. Yamazoe, and Y. Teraoka, "Effects of B-site Partial Substitutions of Perovskite-Type on $La_{0.6}Sr_{0.4}CoO_3$ Oxygen Desorption," *J. Mater. Sci. Lett.*, **8**, 995 (1989).

Zhang, H. M., Y. Shimizu, Y. Teraoka, N. Miura, and N. Yamazoe, "Oxygen Sorption and Catalytic Properties of $La_{1-x}Sr_xCo_{1-y}Fe_yO_{3-\delta}$ Perovskite-Type Oxides," *J. Catal.*, **121**, 432 (1990).

Manuscript received Sept. 20, 2001, and revision received Sept. 12, 2002.